REVIEW

The international reference ionosphere today and in the future

**Dieter Bilitza · Lee-Anne McKinnell · Bodo Reinisch ·
Tim Fuller-Rowell**

Abstract The international reference ionosphere (IRI) is
the internationally recognized and recommended standard
for the specification of plasma parameters in Earth's ion-
osphere. It describes monthly averages of electron density,
electron temperature, ion temperature, ion composition, and
several additional parameters in the altitude range from 60 to
1,500 km. A joint working group of the Committee on Space
Research (COSPAR) and the International Union of Radio
Science (URSI) is in charge of developing and improving the
IRI model. As requested by COSPAR and URSI, IRI is an
empirical model being based on most of the available and
reliable data sources for the ionospheric plasma. The paper
describes the latest version of the model and reviews efforts
towards future improvements, including the development of
new global models for the F2 peak density and height, and a
new approach to describe the electron density in the topside
and plasmasphere. Our emphasis will be on the electron den-
sity because it is the IRI parameter most relevant to geodetic
techniques and studies. Annual IRI meetings are the main
venue for the discussion of IRI activities, future improve-
ments, and additions to the model. A new special IRI task
force activity is focusing on the development of a real-time
IRI (RT-IRI) by combining data assimilation techniques with
the IRI model. A first RT-IRI task force meeting was held in
2009 in Colorado Springs. We will review the outcome of
this meeting and the plans for the future. The IRI homepage
is at http://www.IRI.gsfc.nasa.gov.

Keywords Ionosphere · IRI · Empirical model ·
F2 peak models · Topside

D. Bilitza (✉)
Space Weather Laboratory, George Mason University, Fairfax,
VA 22030, USA
e-mail: dbilitza@gmu.edu; dieter.bilitza-1@nasa.gov

D. Bilitza
Heliospheric Laboratory, NASA Goddard Space Flight Center,
Greenbelt, MD 20771, USA

L.-A. McKinnell
Hermanus Magnetic Observatory, PO Box 32,
Hermanus 7200, South Africa
e-mail: lmckinnell@hmo.ac.za

B. Reinisch
Center for Atmospheric Research, University of Massachusetts
Lowell, 600 Suffolk Street, Lowell, MA 01854, USA
e-mail: Bodo_Reinisch@uml.edu

T. Fuller-Rowell
CIRES University of Colorado and NOAA Space Weather Prediction
Center, 325 Broadway, Boulder, CO 80305, USA
e-mail: Tim.Fuller-Rowell@noaa.gov

1 Introduction

Empirical models play an important role in all parts of the
Sun–Earth environment. They give the scientist, engineer,
and educator easy access to a condensed form of the avail-
able empirical evidence for a specific parameter, optimally,
being based on all reliable data sources that exist for the
parameter. Examples of such widely used models are the
international geomagnetic reference field (IGRF) model for
Earth's magnetic field (IGRF 2010) and the Mass spectrom-
eter and incoherent scatter (MSIS) model for Earth's atmo-
sphere (Picone et al. 2002). The ionospheric equivalent to
these models is the international reference ionosphere (IRI).
Since initiated by the Committee on Space Research
(COSPAR) and the International Union of Radio Science
(URSI) in 1969, IRI has been steadily improved with newer
data and better modeling techniques leading to the release of
a number of key editions of the model including the IRI-78

(Rawer et al. 1978), IRI-85 (Bilitza 1986), IRI-1990
(Bilitza 1990), IRI-2000 (Bilitza 2001), and IRI-2007 (Bilitza and Reinisch 2008). The model progressed from a set
of tables of representative values to an analytical representation of densities and temperatures on the whole globe. It is a
data-based model, as requested by COSPAR and URSI, and
was developed making use of all available and reliable data
sources for the ionospheric plasma. This includes the worldwide network of ionosondes that has monitored ionospheric
electron densities at and below the F-peak for more than half
a century, the powerful incoherent scatter radars that measure
plasma densities, temperatures, and velocities throughout the
whole ionosphere, but unfortunately only at a few selected
locations (∼8 in operation currently), the topside sounder
satellites that have provided the global distribution of electron density from the satellite altitude down to the F-peak, in
situ satellite measurements of ionospheric parameters along
the satellite orbit, and rocket observations of the lower ionosphere, currently the only reliable method to obtain plasma
parameters in the D-region.

Being an empirical model IRI has the advantage that it
does not depend on the evolving theoretical understanding
of the processes that shape the ionospheric plasma. A good
example is the recently discovered four maxima structure
in the longitudinal variation of F-peak electron density and
ionospheric electron content that was first observed with
IMAGE/EUV observations (Immel et al. 2006), and then
confirmed with data from CHAMP (Lühr et al. 2007) and
TOPEX (Schmidt et al. 2008) and that is thought to be caused
by non-migrating, diurnal atmospheric tides that are, in turn,
driven mainly by weather in the tropics. Although theoretical
models still grabble with including this phenomenon in their
modeling framework, inspection of the longitudinal variation of the F-peak density value *NmF2* in IRI revealed that
IRI already reproduces this phenomenon (McNamara et al.
2010). The amplitude of these longitudinal variations is generally smaller in IRI than what is observed. However, that is
understandable, because IRI is based on monthly averages
and the averaging process smoothes out some of these longitude structures.

A disadvantage of empirical models is the strong dependence on the underlying data base. Regions and time periods
not well covered by the data base will result in diminished
reliability of the model in these areas. So, for example, the
representation of the F-peak density (*NmF2*; see Sect. 4) in
IRI is based on the data from the global network of ionosondes. The model performs best at continental northern midlatitudes because that is the region with the highest density
of ionosondes stations and many of these stations have been
operating over a long time period. Most difficult are the ocean
areas, where only a few island stations exist and an interpolation scheme has to be applied to cover this part of the globe.
The two major models in use for *NmF2*, the CCIR (1966)

and URSI-88 (Rush et al. 1989), differ primarily in the interpolation scheme used for the ocean areas. IRI offers use of
both models and based on the data background recommends
the CCIR model for the continents and the URSI-88 model
for the ocean areas. A radically new modeling approach for
this important parameter will be described in Sect. 4 of this
paper.

The main venue for improvements of the IRI model are
annual workshops during which the latest results are presented and discussed and decisions are made regarding model
updates and additions. A new effort was started in 2009 that
has as its goal the development of the real-time IRI (RT-IRI).
A first RT-IRI meeting was held at the US Air Force Academy in Colorado Springs, Colorado, USA in May 2009. The
results from the meeting and plans for the future regarding
this activity will be discussed in Sect. 6.

2 IRI relevance to geodetic techniques

From the start applications of the model have been an important driver for the IRI development and improvement activities. IRI applications range across a wide user community and
this importance was recognized by the International
Standardization Organization (ISO) by voting it the recommended technical specification for ionospheric parameters
(ISO 2009). Here, we will focus on applications of IRI in
the realm of geodetic techniques. We will also discuss the
potential impact of ionospheric data deduced from geodetic
techniques towards improvements of IRI.

One important role of IRI is as a background ionosphere
for validating the reliability and accuracy of a particular
approach for deducing ionospheric parameters from geodetic
measurements. Hernandez-Pajares et al. (2002) and Niranjan et al. (2007) have used IRI for testing algorithms that
convert GPS measurements into global total electron content (TEC) maps. Many tomographic techniques and radio
occultation inversion algorithms got their real first test in an
IRI background ionosphere (Bust et al. 2004; Lee et al. 2008;
Garcia and Crespon 2008). Starting out with an IRI ground
truth ionosphere, the simulated geodetic measurements are
computed for this ionosphere and than the tomographic algorithm is applied to reconstruct the underlying ionosphere,
which is then compared against the original IRI ground truth.
Hocke and Igarashi (2002) used the same approach to validate
their GPS/MET occultation measurement algorithm and Dear
and Mitchell (2006) for testing their MIDAS GPS technique.
Most of these techniques rely on an iterative mathematical process and many use IRI to define the initial conditions for this process (e.g., Bust et al. 2004). Another area
where IRI has helped these techniques is with interpolating in regions where no GPS measurements are available
(e.g.,Orús et al. 2002). Interesting also is the work of

Datta-Barua et al. (2008), who estimated the range of high-order ionospheric errors for the dual-frequency GPS user based on an IRI ionosphere.

Global TEC maps represent the vertical TEC while GPS measurements provide the slant TEC along the path from ground station to satellite. Conversion from slant TEC to vertical TEC is in most cases performed using a thin shell approach which assumes that the ionospheric plasma is compressed into a thin shell at height h_{ts}. The conversion factor depends on the elevation angle of the slant path and on h_{ts}. Many techniques still use a constant (often 300 km) height h_{ts} for this conversion, even though it has been shown that using the varying height of maximum density from IRI, *hmF2* produces superior results (Komjathy et al. 1998; Brunini et al. 2003).

Ionospheric parameters deduced from geodetic measurements are an excellent resource for improving the IRI model. Of greatest interest are electron density profiles deduced through tomography and occultation. Validation of these techniques is progressing successfully, but a few open questions still remain regarding inherent limitation of these techniques in regions of steep gradients and areas of sparse ground station coverage (e.g., the ocean areas). Integral measurements (TEC), on the other hand, are widely used for space weather applications and only a few small issues remain having to do with the inherent instrument bias (Garner et al. 2008) and the conversion algorithm as noted earlier in this section. Bias uncertainties remain also for vertical TEC measurements from dual altimeter instruments like TOPEX, Jason and ERS. Altimeter data complement the GPS data because they provide TEC over the oceans, but not over land. They are an excellent data source for model validations, especially in relation to the relative variation of model parameters thus avoiding bias uncertainties.

Komjathy et al. (1998) were one of the first to assimilate global TEC maps deduced from GPS measurements into the IRI model and thus updating the monthly average model to the daily and hourly ionospheric conditions monitored by GPS. An even more direct approach by Hernandez-Pajares et al. (2002) made use of individual slant TEC measurements. They determine an equivalent solar index by adjusting IRI-slant-TEC to the measured slant-TEC and than use IRI with this modified solar index. More recently, Schmidt et al. (2008) and Zeilhofer et al. (2009) have developed a 4-D representation of the ionospheric electron density using IRI as reference model and using an expansion in B-spline functions to describe the difference term between the reference model and the data (see article by Dettmering et al. in this issue). Other IRI-GPS assimilation schemes have been developed by Fuller-Rowell et al. (2006) using IRI deduced EOF functions to represent TEC over the continental USA (US-TEC) and by Angling et al. (2009) using IRI and GPS data in their electron density assimilative model (EDAM).

3 Status and plans

The newest version of the IRI model, IRI-2011, will include significant improvements not only for the representations of electron density, but also for the description of electron temperature and ion composition. These improvements are the result of modeling efforts, since the last major release, IRI-2007. Modeling progress is documented in several special issues of Advances in Space Research: Volume 39, Number 5, 2007; Volume 42, Number 4, Aug 2008; Volume 43, Number 11, June 2009; Volume 44, Number 6, September 2009.

Our focus here will be only on those improvements that will have an impact on the electron density which is the parameter of most interest for geodetic techniques and data analysis. One of the most important changes is the inclusion of new neural network-based models for the point of highest density which are explained in Sect. 4.

In the bottomside the IRI electron density profile is normalized to the E and F2 peaks and the shape of the profile is determined by the bottomside thickness parameter B_0 and the shape parameter B_1. Currently, two options are given for these parameters: (i) the standard option consisting of a table of values and associated interpolation scheme (Bilitza et al. 2000) and (ii) the Gulyaeva option based on the model of Gulyaeva (1987) utilizing the half-density point $h_{0.5}$ where the topside density has dropped down to half the peak density. Shortcomings of these older models are their limited data base and the resulting misrepresentation of variations with season, latitude and solar activity. Altadill et al. (2008, 2009) have applied spherical harmonic analysis to data from 27 globally distributed ionosondes stations obtaining a new model for B_0 and B_1 that more accurately describes the observed variations with latitude, local time, month, and sunspot number. Overall, the improvements over the older IRI model are of the order of 15–35%. The largest improvements are seen at low latitudes.

At high-latitudes the off-set of the magnetic pole from the geographic pole and its rotation around the geographic (rotation axis) pole together with the influx of energetic solar wind particles results in the formation of the auroral oval at the boundary between closed and open magnetic field lines. Ionospheric densities and temperatures exhibit characteristic variations in and near the oval region and, therefore, the inclusion of an oval description in IRI has long been a high priority of the IRI team (e.g., Szuszczewicz et al. 1993 and Bilitza 1995) and is the first step towards including high-latitude characteristics in IRI. Zhang and Paxton (2008) have recently developed a model of the auroral electron energy flux based on the global far ultraviolet (FUV) measurements with the global ultraviolet imager (GUVI) on the thermosphere ionosphere mesosphere energetics and dynamics (TIMED) satellite. The model also describes the expansion of the oval during magnetic storms. Using a threshold flux value

Zhang et al. (2010) define the poleward and equatorward boundaries of the oval and their movement with magnetic activity. This boundary parameterization is now scheduled for inclusion in IRI.

During night time infrared emissions measured by another TIMED instrument, the sounding of the atmosphere using broadband emission radiometry (SABER) instrument, will help us to represent in IRI the storm induced enhancements of the E-region electron density that is caused by increased particle precipitation. Mertens et al. (2007) and Fernandez et al. (2010) have developed a model for the E-peak enhancement for different levels of magnetic activity using a formalism similar to the one used in the F-region STROM model of Fuller-Rowell et al. (2000). Comparisons with incoherent scatter radar measurements show good agreement (Fernandez et al. 2010).

In addition, IRI-2010 will make use of the latest version of the International Geomagnetic Reference Field (IGRF 2010) for its computation of magnetic coordinates.

These changes will result in significant improvements of IRI electron densities and total electron content (TEC) and, therefore, will benefit the many applications of the IRI model for geodetic techniques and data analysis.

4 New global models for the F2 peak parameters

The point of highest density in the ionosphere, the F2 peak, is defined by two parameters the peak height (*hmF2*) and the peak plasma frequency (foF2) which is directly related to the square-root of the F2 peak density. A third parameter also of interest here is the propagation factor M(3000)F2, which can be monitored from the ground with the help of ionosondes and which is inversely related to *hmF2*. Currently, new neural network (NN) based global models for the F2 peak parameters (foF2 and M(3000)F2) are being developed and evaluated as a possible replacement for the CCIR (1966) and URSI (Rush et al. 1989) models presently used as IRI F2 peak parameter prediction tools. The NN is the technique, whereby a computer is trained to learn the relationship between a given set of inputs and a known output. This technique is very useful in predicting non-linear relationships, and makes use of the history of what has come before. Therefore, it is crucial to have a large database of archived data from which to develop the NN based model. The NNs used in this work make use of the feed forward back propagation algorithm and the reader is referred to Haykin (1994) for more details on the working of NNs.

4.1 foF2 model

Initially, a global foF2 model was developed using hourly values of foF2 from 85 global ionospheric stations, spanning the period 1995–2005 and for a few stations from 1976 to

1986. Data from various resources of the World Data Centre (WDC) archives (Space Physics Interactive Data Resource SPIDR, the Digital Ionogram Database, DIDBase, and IPS Radio and Space Services) have been used in the development of the model. To satisfy all requirements for the model, data from all latitude regions with different levels of magnetic and solar activity and season were used to test for the predictive ability of the NN model and the results were compared with the URSI and CCIR predictions of the IRI model. As shown in Oyeyemi and McKinnell (2008), a large percentage of the data used is from the northern hemisphere, while few of the data are from the southern hemisphere with not much around the equatorial region. A significant paucity of data from the polar sectors (north and south) was also found. The database consisted of a mixture of manually edited and automatically scaled data. Because it was too man-hour intensive to manually edit all of the data, a general trend analysis was performed on all of the data to ensure that there were no extreme outliers and obvious defects in the scaling. The NN technique is able to cope with minor problems in the data in that the technique aims for the best average solution, and will ignore a few serious outliers. The final NN input space for the first version of the foF2 global model consisted of day number, universal time, solar zenith angle, solar activity, magnetic activity, day-of-year, geographic latitude, magnetic inclination and declination. For detailed information on the inputs to the NN the reader is referred to Oyeyemi (2005) and Oyeyemi et al. (2005).

The NN model for predicting the global foF2 value has been tested extensively to judge its ability to meet the requirements for the replacement of the IRI foF2 maps. Figure 1 shows the bar graphs illustrating the RMSE differences between observed foF2 values and predictions by the NN model and the IRI model (URSI and CCIR coefficients) for the foF2 hourly values for a few stations. Further discussion on the testing procedure can be found in McKinnell and Oyeyemi (2009).

Currently, work is progressing on the development and evaluation of this model. Additional data have been acquired to address the gaps in the distribution, particularly at the polar and equatorial regions, and this data will be added to the database and the NN re-trained. The input space is also being assessed since the current input space is not compatible with the current IRI code, and a more compatible input space is required. At each stage of the development, the model is tested and compared with IRI to ensure that the replacement solution for the foF2 maps predicts to a greater accuracy than the current IRI solution.

4.2 M(3000)F2 model

Similarly to the above-described method for developing a new foF2 model, a model for the M(3000)F2 parameter has
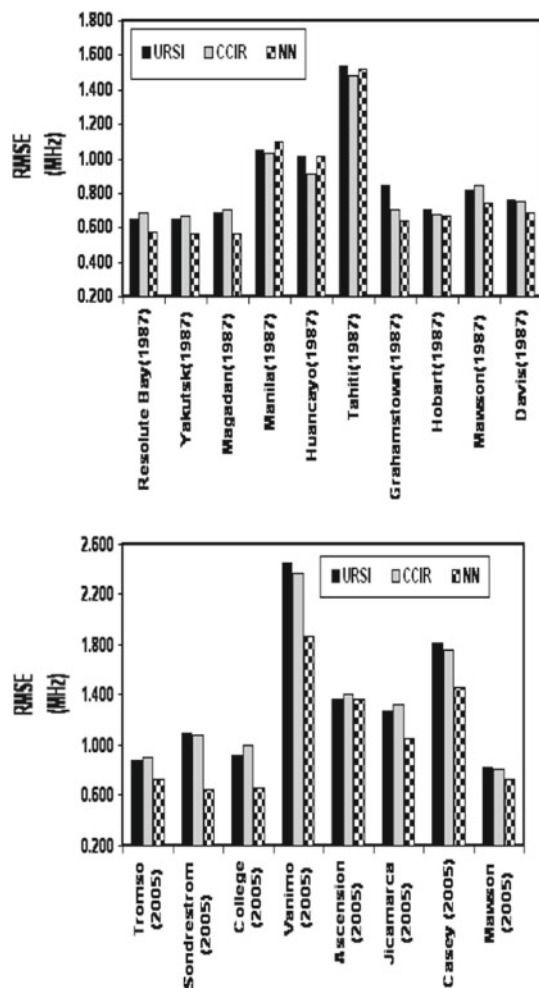
Fig. 1 *Bar graph* illustrations of RMSE differences between observed and URSI, CCIR and NN model predictions for all daily hourly values of foF2 for each verification station for the years indicated (after Oyeyemi and McKinnell 2007)

been developed using the NN technique. A total of 51 global stations were used to create a database of hourly M(3000)F2 values from the period 1964–1986. The original development of this model, which made use of the same input structure as the foF2 model is described in Oyeyemi (2007). Recently, a new version of the M(3000)F2 model was produced with a modified input space that was designed to more easily integrate with the existing IRI code. This modified M(3000)F2 model was presented at the IRI 2009 meeting in Kagoshima, Japan. The model has two major differences to the original version; (i) the magnetic inclination, magnetic declination and angle of meridian were replaced with the modip angle, and (ii) the sunspot number index was replaced with the P10.7 solar flux index. The modip angle was calculated using the IGRF model as is done in IRI. The P10.7 index is calculated as the average of the combination of the daily value of the F10.7 cm flux and the 81 day (3 solar

rotations) running mean of the F10.7 cm radio flux value (F10.7$_{81}$).

Figure 2 shows the measured and predicted M(3000)F2 values for selected example stations and years using the current version of the global model at 10h00 UT. The examples have been chosen to show the prediction ability of the new model for the three latitude zones (equatorial, mid and high) value. Improvements of the IRI predictions vary according to latitude which is expected due to the limited representation of some latitudes within the database. In general, the conclusion was that the new input space variables did not make a significant difference and, therefore, will be taken as the chosen input space for the global peak parameters model due to its compatibility with the existing IRI code.

4.3 Future work

Although the intention is to also develop a global model for *hmF2*, this work is still in the early stages. Variability studies over the Southern African region have been undertaken (Adewale et al. 2009), and a major study has commenced involving various stations around the globe. The global study involves accessing data from various stations, performing a general trend analysis on the data, and creating a database of *hmF2* values that can be used for developing the model.

Regarding the foF2 model, the current version is being updated to accommodate additional data for the polar and equatorial regions that were acquired recently. At the same time, new input space variables will be incorporated into the foF2 model along similar lines as was done for the new version of the M(3000)F2 global model.

Extensive tests on the suitability for inclusion of these models into IRI as replacement modules for the current peak parameter prediction models are being carried out, and the results have been presented at recent IRI workshops. In particular, concerns regarding the predictability of peak parameters at high and equatorial latitudes are being addressed.

5 Representing the topside electron density for IRI

Using newly available satellite data sources, e.g., ISIS-2 and IMAGE/RPI, a new representative model of the topside electron density distribution is being developed. One major challenge for topside N_e modeling is finding a suitable mathematical representation of the topside vertical N_e profiles. Representations that have been proposed include exponential functions (e.g., Bent et al. 1972; Llewellyn and Bent 1973), Epstein function (e.g., Rawer 1988; Radicella and Leitinger 2001; Depuev and Pulinets 2004), Sech-squared function (e.g., Kutiev and Marinov 2007), Chapman function with constant scale height (e.g., Reinisch et al. 2004), Chapman function with two constant scale heights for O^+ and H^+
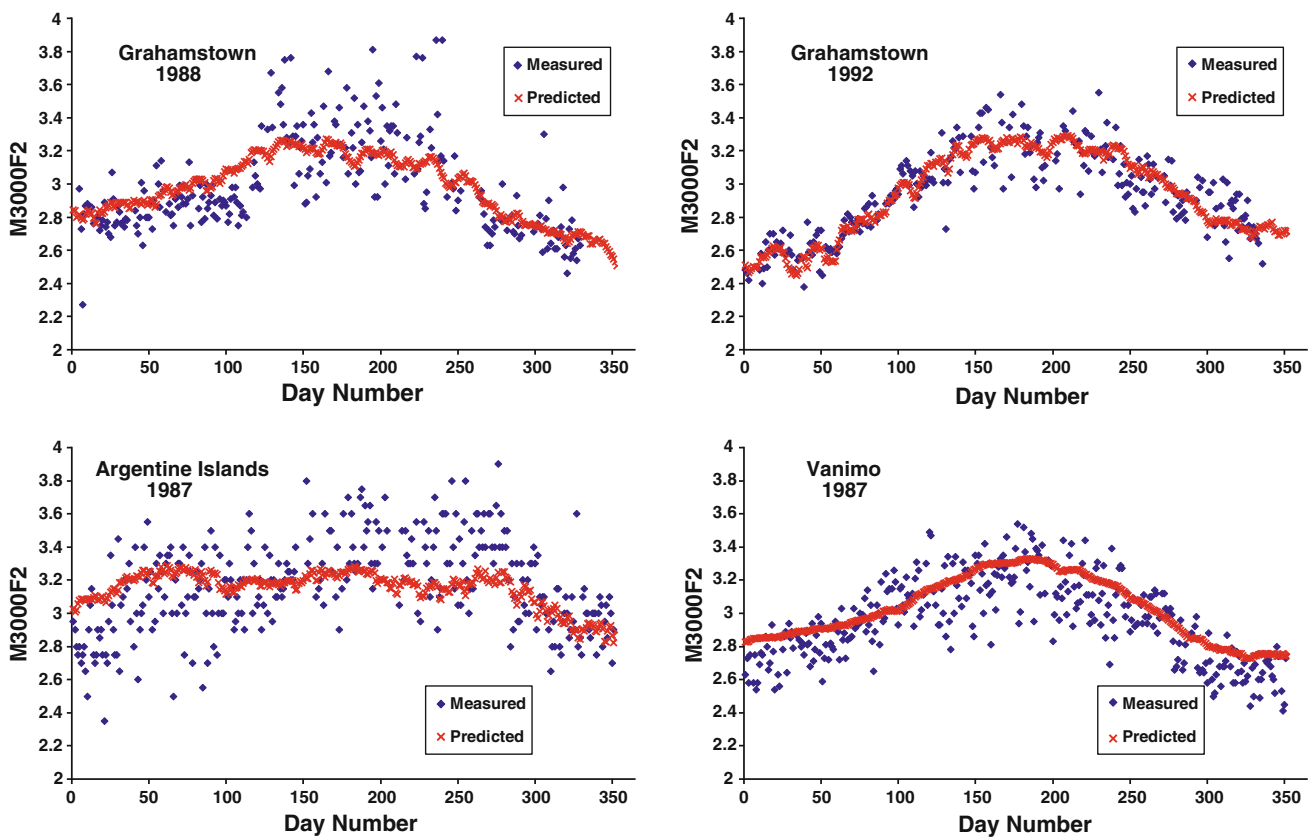
Fig. 2 Measured and predicted M(3000)F2 values for four example stations and years representing three latitude zones at 10h00 UT

(e.g., Kutiev et al. 2006), and the Vary–Chap function (i.e., modified Chapman function for continuously varying scale height) (Reinisch et al. 2007).

The general α-Chapman electron density profile N(h) proposed by Rishbeth and Garriott (1969) has a neutral scale height $H(h)$ that varies with height h, and we, therefore, call it the Vary–Chap function:

$$N_e(h) = N_m \left(\frac{H_m}{H(h)} \right)^{1/2} \exp \left[\frac{1}{2} (1 - y - \exp(-y)) \right],$$

$$y = \int_{h_m}^{h} \frac{dz}{H(z)} \tag{1}$$

where N_m and h_m are the density and height at the F2 peak. Representation of a measured $N(h)$ profile as a Vary–Chap function requires knowledge of $H(h)$. Huang and Reinisch (2001) have shown that Eq. (1) can be solved for $H(h)$ as function of $N(h)$

$$H(h) = H_m \left(\frac{N(h)}{N_m} \right)^{-2} X(h) [1 - \ln X(h)] \tag{2a}$$

where $X(h) = 1 + \frac{1}{H_m} \int_{h_m}^{h} \left(\frac{N(z)}{N_m} \right)^2 dz$ $\qquad$ (2b)

It is easy to show that for H to be real and positive for all $h > h_m$ the value for H_m must satisfy the condition $H_m \geq 0.6 \int_{h_m}^{h_s} [N(z)/N_m]^2 dz$ and in our analysis we selected $H_m = \int_{h_m}^{h_s} [N(z)/N_m]^2 dz$. Here h_s is the height of the satellite; $h_s \approx 1,400$ km for the ISIS-2 satellite. Figure 3 illustrates the duality relation of $N(h)$ and $H(h)$. The left panel shows a measured topside profile (black dots), and the right panel the derived $H(h)$ function. Of course, by inserting this derived $H(h)$ function into Eq. (1), the measured $N(h)$ function is reproduced (red curve in left panel). Of the 80,000 topside electron density profiles obtained from digitized ISIS-2 ionograms (Huang et al. 2002; Bilitza et al. 2004; Benson and Bilitza 2009; Jackson 1969). Reinisch et al. (2007) used all data from magnetically quiet periods ($K_p \leq 3$) to derive median normalized scale height profiles $H_n = H(h)/H_m$ as a function of season, latitude, and local time. The examples in Fig. 4 for the summer at low mid-latitudes show remarkably consistent behavior with not much diurnal variation except that the inter-quartile spread is larger at night as compared to daytime. The normalized scale height function H_n characterizes the shape of the topside profile without dependence on the F2 peak characteristics $hmF2$ and $NmF2$. The $N(h)$ profiles that are calculated from H_n using Eq. (1) are, of course, controlled by these peak values. Because of the large

Fig. 3 *left* ISIS-2 N_e profile (*black dots*), *right* calculated scale height $H(h)/H_m$ profile from the $N(h)$ profile shown on the *left*. The Vary–Chap profile (*red line*) calculated with $H_n(h)$ shown on the *right* is superimposed on the measured profile on the *left*. The two *curves* match so well that they look like a single line
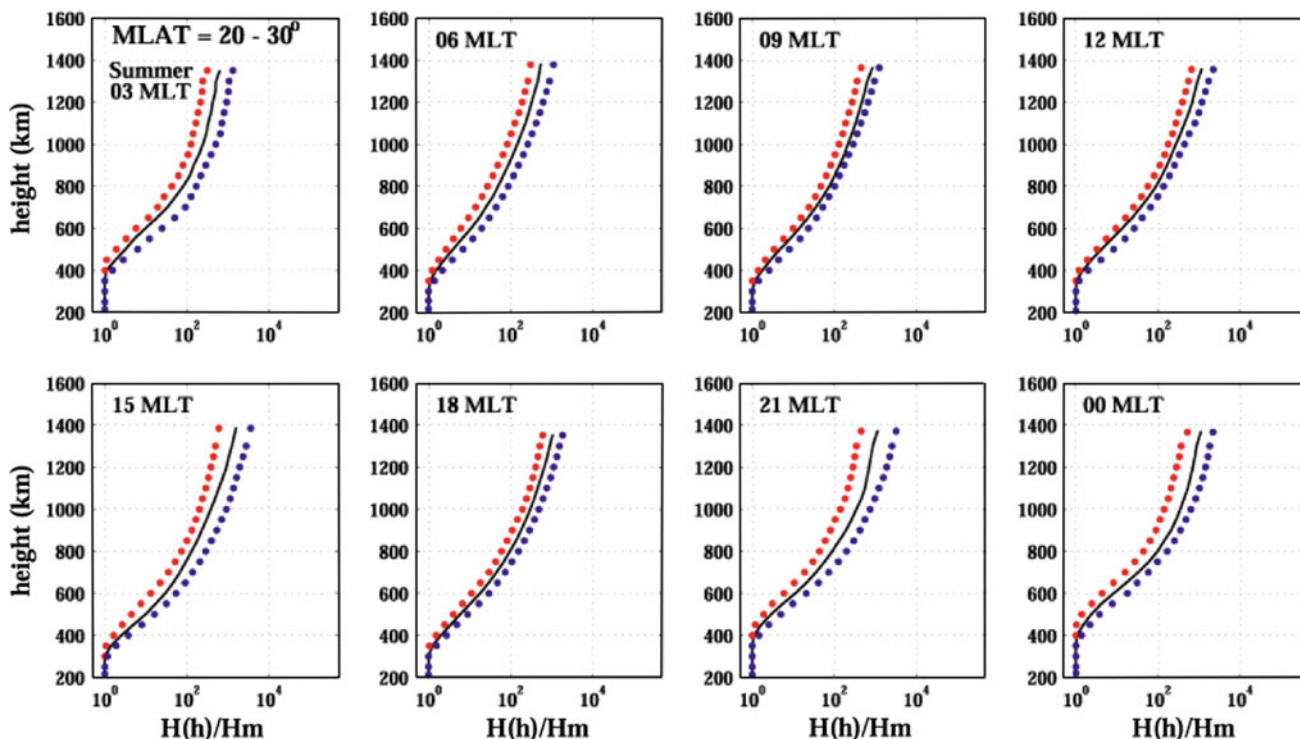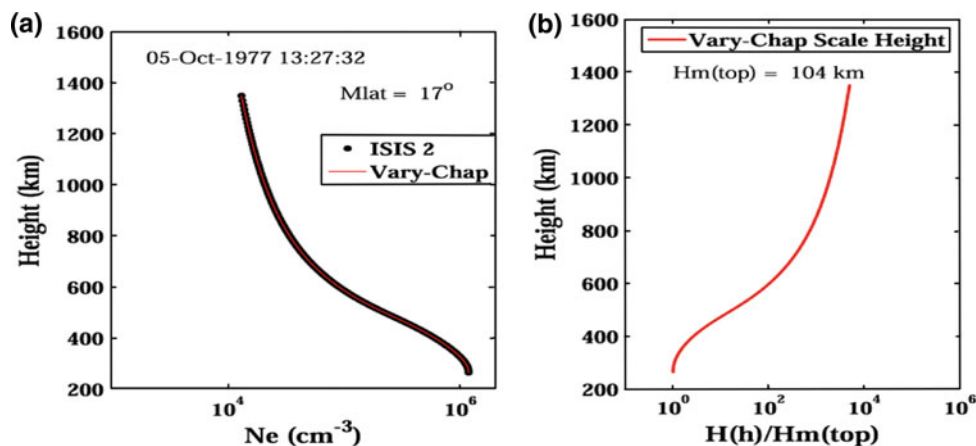

Fig. 4 Median H_n functions (*black line*) for magnetic latitudes between 20° and 30° for summer at different magnetic local times (MLT). The *red* and *blue dots* are the lower and upper quartiles

variation of the F2 peak characteristics, it would not have been meaningful trying to define "median" topside profiles. Nsumei et al. (2010) have used hyperbolic tangent functions for the modeling of $H_n(h)$.

A transition function is used to extend the topside profile to plasmaspheric heights. In Fig. 5a, the measured bottomside profile is extended to the topside using the Vary–Chap topside model constructing the profile up to 1,400 km. The empirical plasmasphere model derived from IMAGE/RPI measurements (Reinisch et al. 2001a,b; Huang et al. 2004) gives the $N(h)$ profile for this location and time in the altitude range

from 2,500 to 4,000 km. Suitable transition functions have been developed that seamlessly connect the ionosphere and plasmasphere profiles as illustrated in Fig. 5b (Reinisch et al. 2007).

6 Real-time IRI

IRI has traditionally been designed to represent the average behavior of the ionosphere at a given place and time, for given levels of solar and geomagnetic activity. The model is not

Fig. 5 **a** The Vary–Chap topside model (with quartiles) extends the measured bottomside profile to 1,400 km altitude. RPI plasmasphere model profile for the same location and time for altitudes above 2,500 km. **b** Connecting a Vary–Chap topside profile (*solid black line*) to the RPI plasmasphere profile (*dashed black line*). *Green line* is IRI model
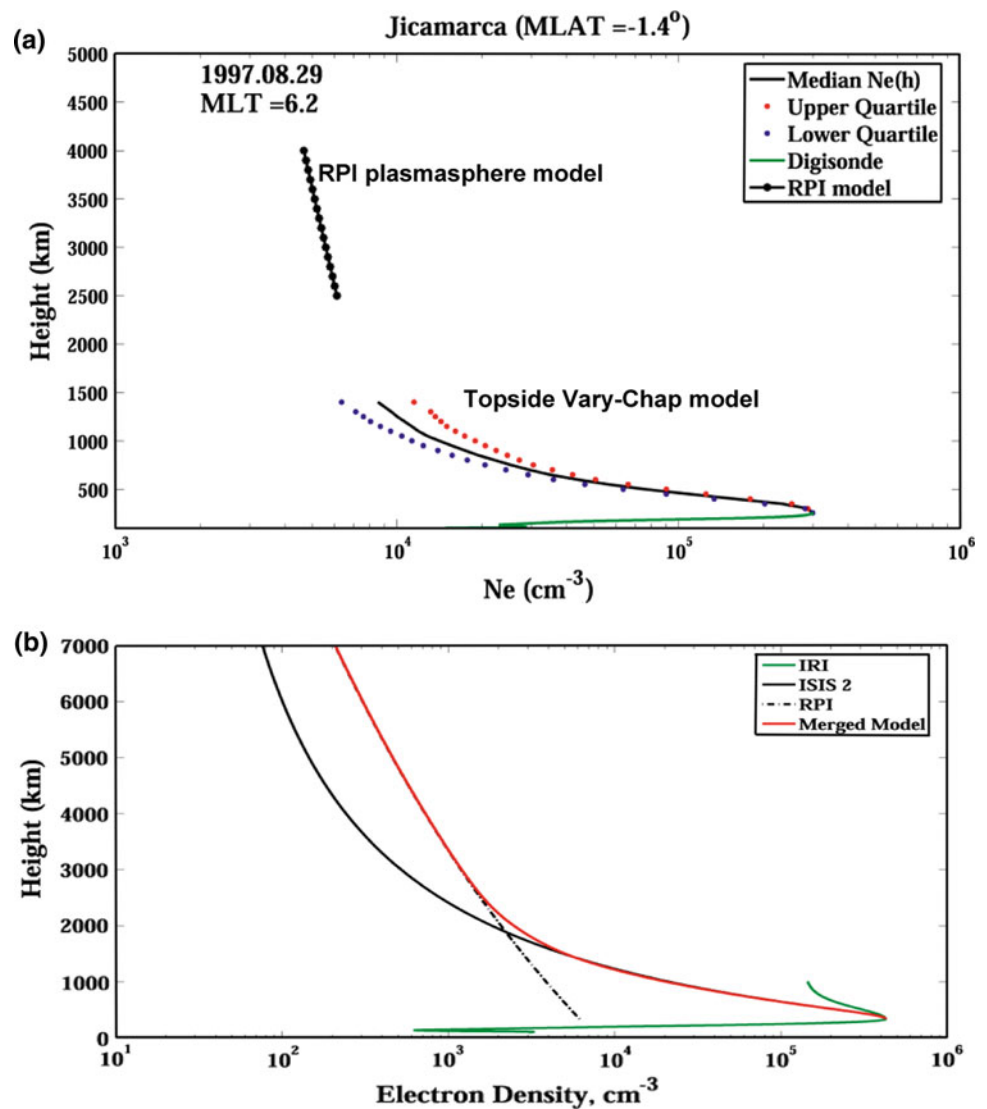

currently designed to predict day-to-day variability beyond that characterized by the indices. For some parameters (e.g. *NmF2*), models have been proposed for IRI that describe estimates of uncertainty or variability in the predicted values (Araujo-Pradere et al. 2005). These uncertainties are based on the standard deviation about the fit to the data, so are unable to characterize whether a particular day is likely to be higher or lower than climatology at any given location. A workshop was held at the Air Force Academy in Colorado Springs 6–8 May 2009 (http://www.ionospheres.org/rtiri2009/) to discuss the feasibility of transitioning from IRI as a climatological reference model to IRI as an ionospheric weather model. The workshop discussed two related, but distinct objectives of the concept of "real time". The first is to provide an historical record of the state of the ionosphere. This post-processing activity does not strictly require the analysis to be done in real time, but is more akin to the concept of "re-analysis" that has been applied to tropospheric weather (Kalnay

et al. 1996), where the operational data assimilation procedure is re-calculated for past years. The re-analysis is usually triggered by new analysis techniques and the need to re-do previous analyses to ensure a continuous improved uniform record. The second objective is to perform the assimilation in real time, pushing the IRI climatological state towards the actual state using all available observations. The two activities are related because they are built upon the same concept, to combine model and data with data assimilation techniques.

There are several motivations for these two activities. Providing an accurate record of the state of the ionosphere over an extended period would contribute a tremendous resource for scientific studies. There is also the need for real-time ionospheric specification and forecast for space weather applications. Using IRI at the heart of a real-time data assimilation system, it utilizes the huge investment over the years to develop an internationally recognized ionospheric reference model, IRI. The activity is timely due to the recent

Fig. 6 Illustration of the significant deviation of ionospheric weather from climatology. The figure shows on the *left* an example of a TEC map that is close to IRI reference climatology. The map on the *right* shows the following day, when the structure is very different from climatology, as produced by the assimilation of GPS data
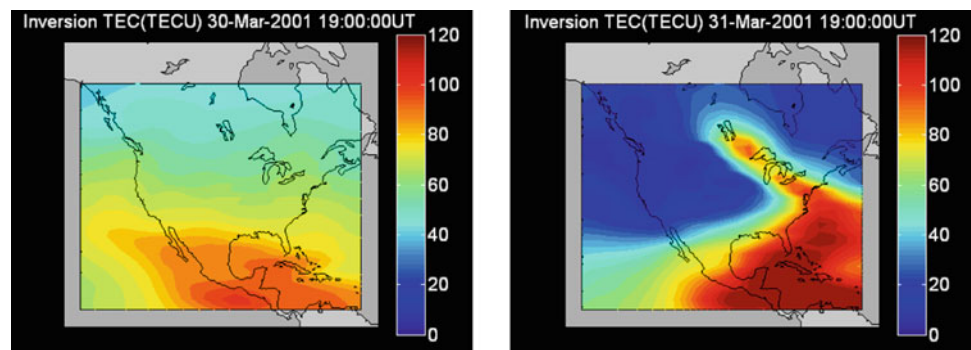
development of data assimilation techniques in the space weather discipline, and the ever increasing availability of ionospheric data from ground and space-based observations, a significant portion of which are available in real time. The motivation has been reinforced further by the increasingly closer connection between meteorology (terrestrial weather) and space weather.

Advances in specification and forecasting troposphere weather has come from the larger increase in the availability of data (primarily from new satellite observations) and the ability to combine the information with a model using optimal data assimilation techniques. The number of real-time ionosondes is increasing (Reinisch and Galkin 2010) and data are available from an ever-increasing global network of dual-frequency GNSS receivers providing slant path electron content. Data are also available from constellations of satellites providing a dense global distribution of radio occultation measurements. The promise of increasing real-time data sources has spawned the development of data assimilation techniques by the space physics community. Two of the early thrusts in this area proceeded under a MURI program, with teams at Utah State University (USU) and the University of Southern California (USC) both using the same acronym: GAIM. The GAIM acronym stood for either Global Assimilation of Ionospheric Measurements in the USU team (Schunk 2004; Scherliess et al. 2006), and Global Assimilative Ionospheric Model in the USC team (Wang et al. 2004; Komjathy et al. 2010).

There are now several operational centers that have adopted data assimilation techniques for ionospheric specification. Maps of real-time TEC for Australia, North America, Europe, and Japan are provided by the Australian Ionospheric Prediction Service (IPS, http://www.ips.gov.au/Satellite/2/1). Other examples are the MIDAS GPS system (Dear and Mitchell 2006) and the EDAM- GPS system (Angling et al. 2009). NOAA's Space Weather Prediction Center (SWPC, http://www.swpc.noaa.gov/) transitioned a regional ionospheric data assimilation model to specify total electron content (TEC) over the contiguous United States (CONUS). The US-TEC model (Fuller-Rowell et al. 2006 uses a real-time network of about 100 ground-based, dual-frequency,

GPS receivers operated by the US Coast Guard, which are part of the Continuously Operating Reference Stations (CORS) network. The data is combined with an empirical ionospheric reference model using a Kalman filter. One of the important aspects of US-TEC is that the reference model is the IRI. Two examples of the TEC maps are shown in Fig. 6 illustrating the significant deviation of ionospheric weather from climatology that can arise. The figure shows on the left, an example of a TEC map that is close to the IRI reference climatology. The map on the right shows the following day during a storm, when the structure is very different from the climatology. These very large deviations from climatology are not typical but do occur during storms; normal day-to-day variability would tend to be smaller. The STORM model in IRI (Fuller-Rowell et al. 2000), which uses the time history of the geomagnetic index Ap, is not able to capture this type of structure. One of the goals of the RT-IRI is to be able to provide this type of information regionally and globally, and not only for TEC, but for all ionospheric parameters, now and for the recent past. The air force weather agency (AFWA), on the other hand, is currently running the USU global Gauss–Markov GAIM model. Other operational centers, such as the international GNSS service (IGS) have chosen to average four different ionospheric data assimilation models to characterizing the ionosphere. IGS require the ionosphere specification for second-order corrections for global navigation and positioning applications (Orús et al. 2002).

The workshop participants, representing activities in 11 countries, reviewed past activities in this area, including the range of data assimilation techniques, some of which are being employed in the operation centers. These include Gauss-Markov Kalman filters, Ensemble Kalman filters, and 3-D and 4-D variational techniques (Kalman 1960; Daley 1991). The participants also reviewed the available data sources suitable for use by a RT-IRI initiative, and the important issue of data quality and error estimation. One of the important components of data assimilation is the need to have accurate estimates of observation error, which in the past have been poorly quantified.

The consensus of the participants was that the initial focus of the Task Force should be on regional retrospective

analysis for selected periods, and eventually combine the regions to produce a global specification in real time. The parameters chosen to target were the 2-D maps of *NmF2*, *hmF2*, and TEC, plus estimates of uncertainty, gradually migrating to the 3D ionospheric structure later. The data chosen for this first study would include hand-scaled ionograms and ground-based GNSS receivers. Just as in tropospheric numerical weather prediction (NWP), new datasets will be added after careful evaluation of their impact on the analysis (Cucurull et al. 2006). This will include radio occultation data from the COSMIC satellite constellation (Anthes et al. 2008). In the future, the assimilation period will be extended and the results made available to the community on the IRI web page for scientific studies. The group will also explore methodologies to combine the regional maps to produce a global high-resolution analysis, recognizing the limitations in the accuracy in data sparse regions. The availability of space based radio occultation data will be particularly important to improve the accuracy over the oceans.

7 Conclusions

We have presented the current status of IRI modeling activities and plans for the future with special emphasis on the parameters and regions that are most important for geodetic measurement techniques and their data analysis schemes. IRI and geodetic techniques have benefitted each other. We have presented many examples of applications of IRI in geodetic techniques. This includes the use of the height of largest density from IRI for the conversion of slant GPS-TEC to vertical TEC. IRI has been widely used as a background model to test tomographic and radio occultation algorithms related to signals from high and low orbiting GPS satellites. In turn ionospheric measurements from geodetic techniques are a promising new resource for improvements of IRI and an excellent candidate for data assimilation into the IRI model. With data assimilation the IRI model can progress from the monthly average conditions (climatology) that it is representing now to daily and hourly conditions if a good set of global observations is available. The ultimate goal is the development of a Real Time IRI that assimilates all available and reliable ionospheric measurements into the model including ionosonde and incoherent scatter radar measurements from below, satellite in situ measurements from within, and GPS and radio occultation measurements from above. The IRI community is ideally suited to perform this new extension to the capabilities of this internationally recognized ionospheric reference model. The IRI science community has a long history of working together efficiently and productively. With the increase in the number of data sources and the development of data assimilation techniques in the ionospheric community this is the right time to make this important advance,

and follow the lead from the tropospheric weather forecasting community.

References

Adewale AO, Oyeyemi EO, McKinnell LA (2009) Comparisons of observed ionospheric F2 peak parameters with IRI-2001 predictions over South Africa. J Atmos Solar Terr Phys 71(2):273–284. doi:10.1016/j.jastp.2008.10.014

Altadill D, Arrazola D, Blanch E, Buresova D (2008) Solar activity variations of ionosonde measurements and modeling results. Adv Space Res 42:610–616. doi:10.1016/j.asr.2007.07.028

Altadill D, Torta JM, Blanch E (2009) Proposal of new models of the bottom-side B0 and B1 parameters for IRI. Adv Space Res 43:1825–1834. doi:10.1016/j.asr.2008.08.0144

Angling M, Shaw J, Shukla A, Cannon P (2009) Development of an HF selection tool based on the Electron Density Assimilative Model near-real-time ionosphere. Radio Sci 44:RS0A13. doi:10.1029/2008RS004022

Anthes RA, Ector D, Hunt DC, Kuo Y-H, Rocken C, Schreiner WS, Sokolovskiy SV, Syndergaard S, Wee T-K, Zeng Z, Bernhardt PA, Dymond KF, Chen Y, Liu H, Manning K, Randel WJ, Trenberth KE, Cucurull L, Healy SB, Ho S-P, McCormick C, Meehan TK, Thompson DC (2008) The COSMIC/FORMOSAT-3 mission: early results. Bull Am Meteorol Soc 89:313–333. doi:10.1175/BAMS-89-3-313

Araujo-Pradere EA, Fuller-Rowell TJ, Codrescu MV, Bilitza D (2005) Characteristics of the ionospheric variability as a function of season, latitude, local time, and geomagnetic activity. Radio Sci 40:RS 5009. doi:10.1029/2004RS003179

Araujo-Pradere EA, Fuller-Rowell TJ, Spencer PSJ, Minter CF (2007) Differential validation of the US-TEC model. Radio Sci 42:RS3016. doi:10.1029/2006RS003459

Benson RF, Bilitza D (2009) New satellite mission with old data: rescuing a unique data set. Radio Sci 44:RS0A04. doi:10.1029/2008RS004036

Bent RB, Llewellyn SK, Schmid PE (1972) Description and evaluation of the Bent ionospheric model, vol 1–3. National Information Service, Springfield, Virginia AD-753-081,-082,-083

Bilitza D (1986) International reference ionosphere: recent developments. Radio Sci 21:343–346

Bilitza D (1990) International reference ionosphere 1990, NSSDC/WDC-A-R&S 90-22. National Space Science Data Center, Greenbelt

Bilitza D (1995) Including auroral boundaries in the IRI model. Adv Space Res 16(1):13–16

Bilitza D, Radicella S, Reinisch B, Adeniyi J, Mosert M, Zhang S, Obrou O (2000) New B0 and B1 models for IRI. Adv Space Res 25(1):89–95

Bilitza D (2001) International reference ionosphere 2000. Radio Sci 36(2):261–275

Bilitza D, Huang X, Reinisch B, Benson R, Hills HK, Schar WB (2004) Topside ionogram scaler with true height algorithm (TOPIST): automated processing of ISIS topside ionograms. Radio Sci 39(1):RS1S27. doi:10.1029/2002RS002840

Bilitza D, Reinisch BW (2008) International reference ionosphere 2007: improvements and new parameters. Adv Space Res 42(4):599–609. doi:10.1016/j.asr.2007.07.048

Brunini C, Van Zele MA, Meza A, Gende M (2003) Quiet and perturbed ionospheric representation according to the electron content from GPS signals. J Geophys Res 108(A2):1056. doi:10.1029/2002JA009346

Bust GS, Garner TW, Gaussiran TLII (2004) Ionospheric data assimilation three-dimensional (IDA3D): a global, multisensor, electron density specification algorithm. J Geophys Res 109:A11312. doi:10.1029/2003JA010234

CCIR (1966) Atlas of ionospheric characteristics. Report 340-1, 340-6. Comité Consultatif International des Radiocommunications, Genève, Switzerland. ISBN 92-61-04417-4

Cucurull L, Kuo Y-H, Barker D, Rizvi SRH (2006) Assessing the impact of simulated COSMIC GPS radio occultation data on weather analysis over the Antarctic: a case study COSMIC project. Mon Weather Rev 134:3283–3296

Daley R (1991) Atmospheric data analysis. Cambridge University Press, Cambridge

Datta-Barua S, Walter T, Blanch J, Enge P (2008) Bounding higher-order ionospheric errors for the dual-frequency GPS user. Radio Sci 43:RS5010. doi:10.1029/2007RS003772

Dear R, Mitchell C (2006) GPS interfrequency biases and total electron content errors in ionospheric imaging over Europe. Radio Sci 41:RS6007. doi:10.1029/2005RS003269

Depuev VH, Pulinets SA (2004) A global empirical model of the ionospheric topside electron density. Adv Space Res 34:2016–2020

Fernandez JR, Mertens CJ, Bilitza D, Xu X, Russell JMIII, Mlynczak MG (2010) Feasibility of developing an ionospheric E-region electron density storm model using TIMED/SABER measurements. Adv Space Res 46(8):1070–1077. doi:10.1016/j.asr.2010.06.008

Friedrich M, Torkar KM, Lehmacher GA, Croskey CL, Mitchell JD, Kudeki E, Milla M (2006) Rocket and incoherent scatter radar common-volume electron measurements of the equatorial lower ionosphere. Geophys Res Lett 33:L08807. doi:10.1029/2005GL024622

Fuller-Rowell TJ, Araujo-Pradere E, Codrescu MV (2000) An empirical ionospheric storm-time correction model. Adv Space Res 25(1):139–146

Fuller-Rowell T, Araujo-Pradere E, Minter C, Codrescu M, Spencer P, Robertson D, Jacobsen A (2006) US-TEC: a new data assimilation product from the space environment center characterizing the ionospheric total electron content using real-time GPS data. Radio Sci 41. doi:10.10292005RS003393

Garcia R, Crespon F (2008) Radio tomography of the ionosphere: analysis of an underdetermined, ill-posed inverse problem, and regional application. Radio Sci 43:RS2014. doi:10.1029/2007RS003714

Garner TW, Gaussiran TLII, Tolman BW, Harris RB, Calfas RS, Gallagher H (2008) Total electron content measurements in ionospheric physics. Adv Space Res 42(4):720–726. doi:10.1016/j.asr.2008.02.025

Gulyaeva T (1987) Progress in ionospheric informatics based on electron density profile analysis of ionograms. Adv Space Res 7(6):39–48

Haykin S (1994) Neural networks: a comprehensive foundation. Macmillan, New York

Hernandez-Pajares M, Juan J, Sanz J, Bilitza D (2002) Combining GPS measurements and IRI model values for Space Weather specification. Adv Space Res 29(6):949–958

Hocke K, Igarashi K (2002) Structure of the earth's lower ionosphere observed by GPS/MET radio occultation. J Geophys Res 107(A5). doi:10.1029/2001JA900158

Huang X, Reinisch BW (2001) Vertical electron content from ionograms in real time. Radio Sci 36:335–342

Huang X, Reinisch BW, Bilitza D, Benson RF (2002) Electron density profiles of the topside ionosphere. Ann Geophys 45(1):125–130

Huang X, Reinisch BW, Song P, Nsumei P, Green JL, Gallagher DL (2004) Developing an empirical density model of the plasmasphere using IMAGE/RPI observations. Adv Space Res 33:829–832

IGRF (2010) International Geomagnetic Reference Field, Version 11. http://www.ngdc.noaa.gov/IAGA/vmod/igrf.html

Immel TJ, Sagawa E, England SL, Henderson SB, Hagan ME, Mende SB, Frey HU, Swenson CM, Paxton LJ (2006) Control of equatorial ionospheric morphology by atmospheric tides. Geophys Res Lett 33:L15108. doi:10.1029/2006GL026161

ISO (2009) Space environment (natural and artificial)—Earth's ionosphere model: international reference ionosphere and extension to the plasmasphere. Technical Specification TS16457, International Standardization Organization, Geneva, Switzerland

Jackson JE (1969) The reduction of topside ionograms to electron-density profiles. Proc IEEE 57:960–976

Kalman RE (1960) A new approach to linear filtering and prediction problems. Trans ASME J Basic Eng 82:35–45

Kalnay E, Kanamitsu M, Kistler R, Collins W, Deaven D, Gandin L, Iredell M, Saha S, White G, Woollen J, Zhu Y, Chelliah M, Ebisuzaki W, Higgins W, Janowiak J, Mo KC, Ropelewski C, Wang J, Leetmaa A, Reynolds R, Jenne R, Joseph D (1996) The NCEP/NCAR 40-year reanalysis project. Bull Am Meteorol Soc 77:437–471

Komjathy A, Lagnley R, Bilitza D (1998) Ingesting GPS-derived TEC data into the international reference ionosphere for single frequency radar altimeter ionosphere delay corrections. Adv Space Res 22(6):793–802

Komjathy A, Wilson B, Pi X, Akopian V, Dumett M, Iijima B, Verkhoglyadova O, Mannucci AJ (2010) JPL/USC GAIM: on the impact of using COSMIC and ground-based GPS measurements to estimate ionospheric parameters. J Geophys Res 115:A02307. doi:10.1029/2009JA014420

Kutiev I, Marinov P (2007) Topside sounder model of scale height and transition height characteristics of the ionosphere. Adv Space Res 39:759–766. doi:10.1016/j.asr.2006.06.013

Kutiev IS, Marinov PG, Watanabe S (2006) Model of topside ionosphere scale height based on topside sounder data. Adv Space Res 37:943–950. doi:10.1016/j.asr.2005.11.021

Lee JK, Kamalabadi F, Makela JJ (2008) Three-dimensional tomography of ionospheric variability using a dense GPS receiver array. Radio Sci 43:RS3001. doi:10.1029/2007RS003716

Llewellyn SK, Bent RB (1973) Documentation and description of the Bent ionospheric model. Report AFCRL-TR-73-0657, Hanscom AFB, MA

Lühr H, Hausler K, Stolle C (2007) Longitudinal variation of F region electron density and thermospheric zonal wind caused by atmospheric tides. Geophys Res Lett 34:L16102. doi:10.1029/2007GL030639

McKinnell LA, Oyeyemi EO (2009) Progress towards a new global *foF2* model for the international reference ionosphere (IRI). Adv Space Res 43:1770–1775. doi:10.1016/j.asr.2008.09.035

McNamara LF, Retterer JM, Baker CR, Bishop GJ, Cooke DL, Roth CJ, Welsh JA (2010) Longitudinal structure in the CHAMP electron densities and their implications for global ionospheric modeling. Radio Sci 45:RS2001. doi:10.1029/2009RS004251

Mertens C, Winick J, Russell JIII, Mlynczak M, Evans D, Bilitza D, Xu X (2007) Empirical storm-time correction to the international reference ionosphere model E-region electron and ion density parameterizations using observations from TIMED/SABER. Proc SPIE Remote Sens Clouds Atmos 12:67451L. doi:10.1117/12.737318

Niranjan K, Srivani B, Gopikrishna S, Rama Rao PVS (2007) Spatial distribution of ionization in the equatorial and low-latitude ionosphere of the Indian sector and its effect on the Pierce point altitude for GPS applications during low solar activity periods. J Geophys Res 112:A05304. doi:10.1029/2006JA011989

Nsumei P, Reinisch BW, Huang X, Bilitza D (2010) Empirical topside electron density model derived from ISIS satellite sounding data. J Earth Planets Space (submitted)

Orús R, Hernández-Pajares M, Juan JM, Sanz J, García-Fernández M (2002) Performance of different TEC models to provide GPS ionospheric corrections. J Atmos Solar-Terr Phys 64(18):2055–2062

Oyeyemi EO (2005) A global ionospheric F2 region peak electron density model using neural networks and extended geophysically relevant inputs. PhD thesis, Rhodes University, Grahamstown, South Africa

Oyeyemi EO, Poole AWV, McKinnell LA (2005) On the global model for foF2 using neural networks. Radio Sci 40:RS6011. doi:1029/2004RS003223

Oyeyemi EO, McKinnell LA, Poole AWV (2007) Neural network based prediction techniques for global modeling of M(3000)F2 ionospheric parameter. Adv Space Res 39(5):643–650. doi:1016/j.asr.2006.09.038

Oyeyemi EO, McKinnell LA (2008) A new global F2 peak electron density model for the International Reference Ionosphere (IRI). Adv Space Res 42(4):645–658. doi:10.1016/j.asr.2007.10.031

Picone JM, Hedin AE, Drob DP, Aikin AC (2002) NRLMSISE-00 empirical model of the atmosphere: statistical comparisons and scientific issues. J Geophys Res 107(A12):1468. doi:10.1029/2002JA009430

Radicella SM, Leitinger R (2001) The evolution of the DGR approach to model electron density profiles. Adv Space Res 27(1):35–40

Rawer K (1988) Synthesis of ionospheric electron density profiles with Epstein functions. Adv Space Res 8(4):191–198

Rawer K, Bilitza D, Ramakrishnan S (1978) International reference ionosphere 78. Special Report, International Union of Radio Science (URSI), Brussels, Belgium

Reinisch BW, Huang X, Haines DM, Galkin IA, Green JL, Benson RF, Fung SF, Taylor WWL, Reiff PH, Gallagher DL, Bougeret J-L, Manning R, Carpenter DL, Boardsen SA (2001) First results from the radio plasma imager on IMAGE. Geophys Res Lett 28:1167–1170

Reinisch BW, Huang X, Song P, Sales GS, Fung SF, Green JL, Gallagher DL, Vasyliunas VM (2001) Plasma density distribution along the magnetospheric field: RPI observations from IMAGE. Geophys Res Lett 28:4521–4524

Reinisch BW, Huang X, Belehaki A, Shi J, Zhang ML, Ilma R (2004) Modeling the IRI topside profile using scale heights from ground-based ionosonde measurements. Adv Space Res 34:2026–2031. doi:10.1016/j.asr.2004.06.012

Reinisch BW, Nsumei P, Huang X, Bilitza DK (2007) Modeling the F2 topside and plasmasphere for IRI using IMAGE/RPI, and ISIS data. Adv Space Res 39:731–738. doi:10.1016/j.asr.2006.05.032

Reinisch BW, Galkin I (2010) Global ionospheric radio observatory (GIRO). Earth Planets Space (submitted)

Rishbeth H, Garriott OK (1969) Introduction to ionospheric physics. Academic Press, New York

Rush C, Fox M, Bilitza D, Davies K, McNamara L, Stewart F, PoKempner M (1989) Ionospheric mapping—an update of foF2 coefficients. Telecomm J 56:179–182

Scherliess L, Schunk RW, Sojka JJ, Thompson DC, Zhu L (2006) Utah State University global assimilation of ionospheric measurements gauss-markov kalman filter model of the ionosphere: model description and validation. J Geophys Res 111:A11315. doi:10.1029/2006JA011712

Scherliess L, Thompson DC, Schunk RW (2008) Longitudinal variability of low-latitude total electron content: tidal influences. J Geophys Res 113:A01311. doi:10.1029/2007JA012480

Schmidt M, Bilitza D, Shum C, Zeilhofer C (2008) Regional 4-D modeling of the ionospheric electron density. Adv Space Res 42(4):782–790. doi:10.1016/j.asr.2007.02.050

Schunk RW, Scherliess L, Sojka JJ, Thompson DC, Anderson DN, Codrescu MV, Minter Cliff, Fuller-Rowell TJ, Heelis RA, Hairston M, Howe BM (2004) Global assimilation of ionospheric measurements (GAIM). Radio Sci 39:RS1S02. doi:10.1029/2002RS002794

Szuszczewicz E et al (1993) Measurements and empirical model comparisons of F-region characteristics and auroral boundaries during the solstial SUNDAIL campaign of 1987. Ann Geophys 11:601–613

Wang C, Hajj G, Pi X, Rosen IG, Wilson B (2004) Development of the global assimilative ionospheric model. Radio Sci 39:RS1S06. doi:10.1029/2002RS002854

Zeilhofer C, Schmidt M, Bilitza D, Shum C (2009) Regional 4-D modeling of the ionospheric electron density from satellite data and IRI. Adv Space Res 43(11):1669–1675. doi:10.1016/j.asr.2008.09.033

Zhang Y, Paxton LJ (2008) An empirical Kp-dependent global auroral model based on TIMED/GUVI data. J Atmos Solar-Terr Phys 70:1231–1242. doi:10.1016/j.jastp.2008.03.008

Zhang Y, Paxton LJ, Bilitza D (2010) Near real-time assimilation of auroral peak E-region density and equatorward boundary in IRI. Adv Space Res 46(8):1055–1063. doi:10.1016/j.asr.2010.06.029